Expanded View to Weinert *et al*.

Tables

Table I. Overview of features of our ClC-7 mouse models studied previously and in this study.
Green symbols indicate normal properties and red symbols abnormal (pathological) ones. n, normal. Down arrow indicate quantitatively decreased values.

Table I.

	Clcn7 $^{+/+}$	*Clcn7* $^{unc/unc}$	*Clcn7* $^{td/td}$	*Clcn7* $^{-/-}$
Intact protein	+	+	+	–
Electric shunt	+	+	–	–
Cl^-/H^+-exchange	+	–	–	–
Survival	+	–	–(+)	–
Lysosomal pathology	–	++	+	++
Lysosomal pH	n	n	n	n
Lysosomal $[Cl^-]$	n	↓	↓	↓
Osteopetrosis	–	+	++	++
Pigmentation defect	–	–	–	++

Table II. Antibodies used in this study. rb, rabbit; gp guinea pig; IHC, immunohistochemistry; ICC, immunocytochemistry; WB, western blot.

Table II.

	species	source	IHC	ICC	WB
Anti-ClC-7	rb, gp	Kornak et al, 2001	1:100	1:300	1:500
Anti-Ostm1	rb, gp	Lange et al, 2006	1:50	1:150	1:200
Anti-Lamp-1	rb	abcam, # ab24170	1:300	—	—
Anti-Lamp-1	rat	BD Bioscience, # 553792	1:100	1:200	—
Anti-a3 (V- ATPase)	gp	Lange et al, 2006	1:100	—	—
Anti-Actin	rb	Sigma-Aldrich, # A-2066	—	—	1:1000
Anti-LC3	rat	Abgent, # AP1802a	—	—	1:300

Table III. Number of animals/cell lines used for experiments.

Table III.

	number
Figure 1C	3 (+/+,td/td) independent cell lines
Figure 2 A-C	4 (+/+,td/td) animals
Figure 2 D-H	2 (+/+,td/td) animals
Figure 3 A	3 (+/+,td/td,unc/unc) animals
Figure 3 B	2 (td/td) animals
Figure 4 A	5 (+/+), 4 (td/td), 3(–/–) animals
Figure 4 B	2 (+/+,td/td) animals
Figure 4 D,E	2 (+/+,td/td,unc/unc,–/–) animals
Figure 5 A,B	3 (+/+,td/td) animals
Figure E5 A	2 (+/+,td/td,unc/unc,–/–) animals
Figure E5 B	2 (+/+,td/td) animals
Figure E6 A,B	2 (+/+,td/td) animals

Figures

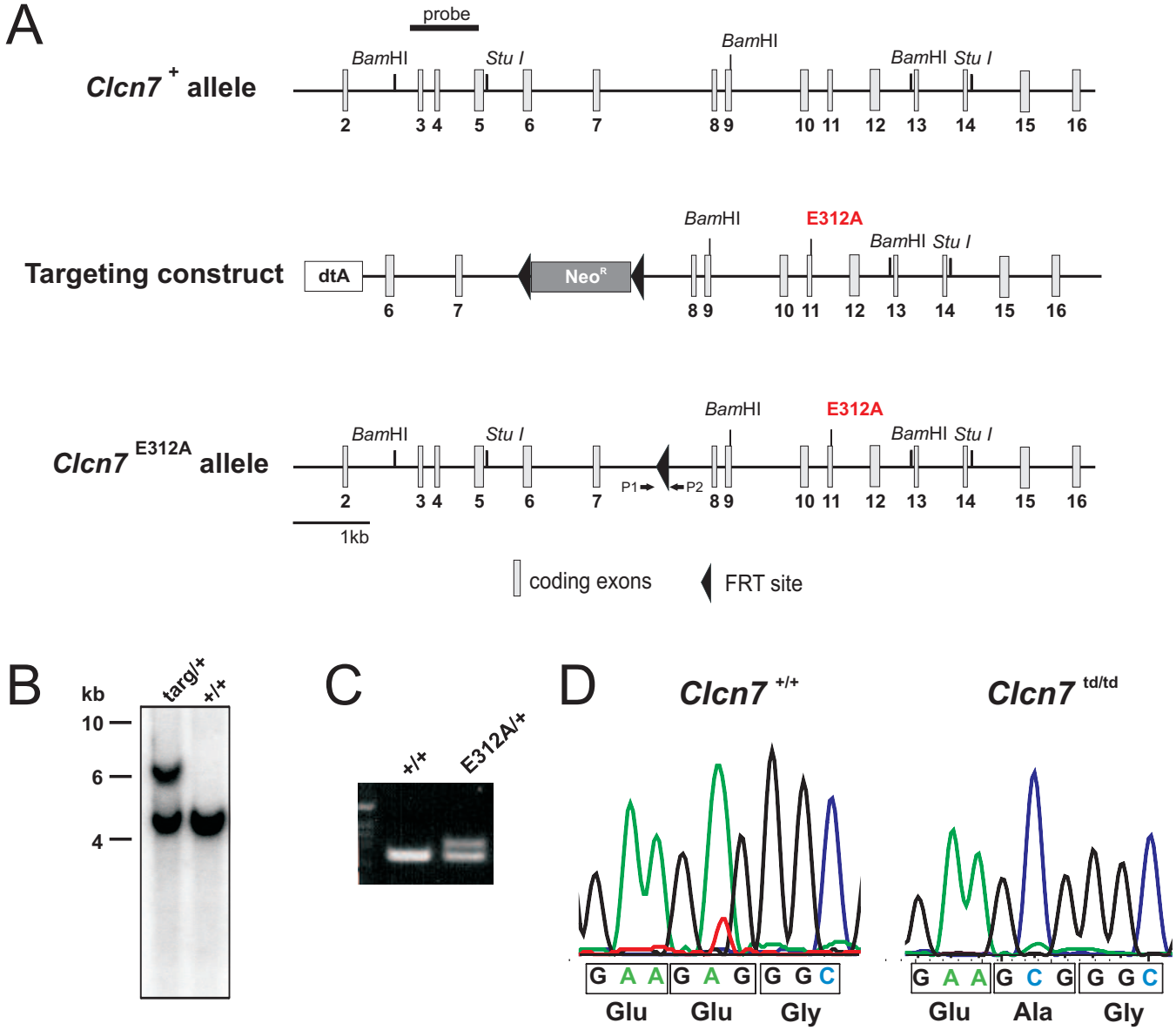

Figure E1. Generation of *Clcn7*$^{td/td}$ mice. (**A**) Gene targeting strategy. Targeting construct contains 8 kb of mouse genomic sequence encompassing exon 6 through 16 with a dtA (diphtheria toxin A) cassette added to one end to select for homologous recombination. We modified Exon 11 by introducing the E312A mutation and inserted a neomycin (Neo^{R}) resistance cassette (flanked by FRT sites) between exons 7 and 8 as selection marker. Correctly targeted embryonic stem (ES) cells were injected into blastocysts. Chimeric animals were crossed with FLPe-recombinase-expressing 'deleter' mice (Rodríguez et al, 2000) resulting in the *Clcn7*^{E312A} allele (bottom). (**B**) Mouse genomic ES cell DNA was digested with *Bam*HI for Southern blot analysis. Positive clones were identified with an external hybridization probe shown in (A). (**C**) PCR on mouse genomic DNA was used for genotyping. The sequences of PCR primers shown in (A) were for P1: 5' TATCTCAGAAGGCAGGTAGG 3' and for P2: 5' AGTCTGTTAGCCAGAGGTAG 3'. (**D**) DNA sequence obtained from homozygous *Clcn7*$^{td/td}$ mice confirmed the presence of the E312A mutation.

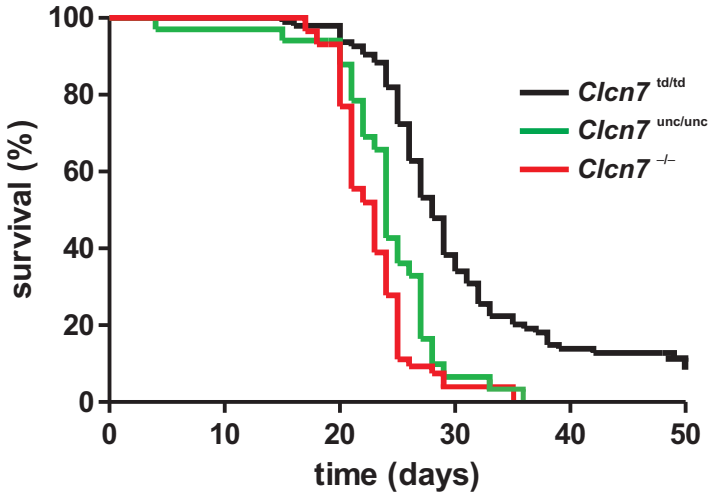

Figure E2. Survival rates of ClC-7 mouse models. *Clcn7*$^{unc/unc}$ and *Clcn7*$^{-/-}$ mice died within 3-4 weeks after birth, whereas *Clcn7*$^{td/td}$ mice died on average a few days later. Intriguingly, some *Clcn7*$^{td/td}$ mice survived for more than 2 months and even got older than 10 months (*Clcn7*$^{td/td}$, n = 103, *Clcn7*$^{-/-}$, n = 61 and *Clcn7*$^{unc/unc}$, n = 35).

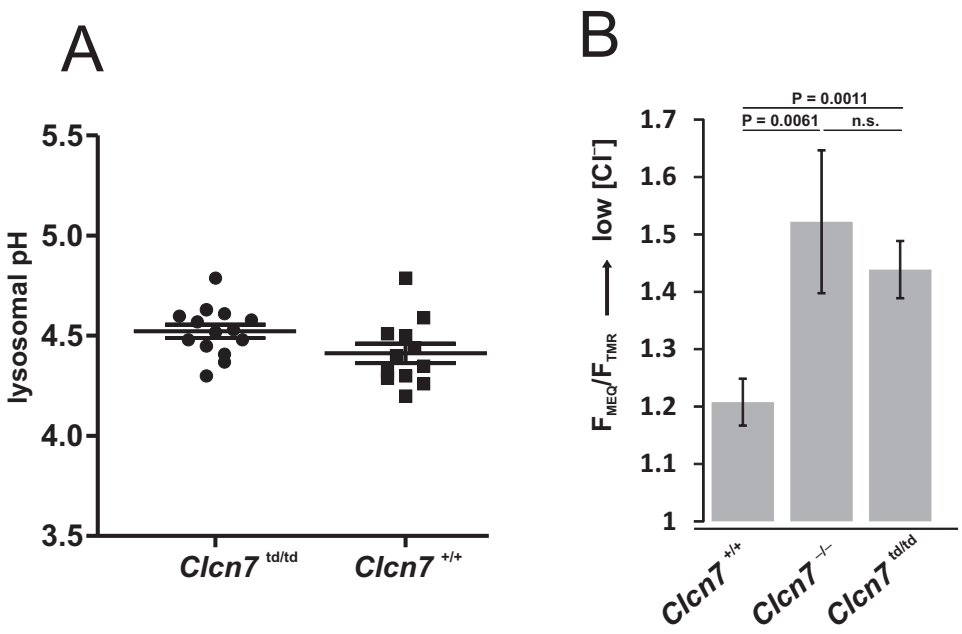

Figure E3. Ion homeostasis in lysosomes in ClC-7 mouse models. (**A**) No significant difference in steady-state lysosomal pH between *Clcn7*$^{td/td}$ and *Clcn7*$^{+/+}$ fibroblasts as measured by Oregon Green dextran fluorescence in 3 independent cell lines and 15 (td/td) and 11 (+/+) dishes. Lines show mean ± s.e.m. of the individual measurements that are depicted as dots and squares. (**B**) Lysosomal chloride concentration was reduced in *Clcn7*$^{td/td}$ compared to WT lysosomes as measured by fluorescence ratio of MEQ over TMR, which were coupled to dextran. Cells were preincubated in low Cl^- saline to shift $[Cl^-]_{lys}$ into the useful measuring range. Means (n=12 for WT and td/td; n= 7 for –/–) from 5 (WT), 2 (–/–) and 6 (td/td) different primary cell lines are shown. Student's t-test was applied, n.s., not significant.

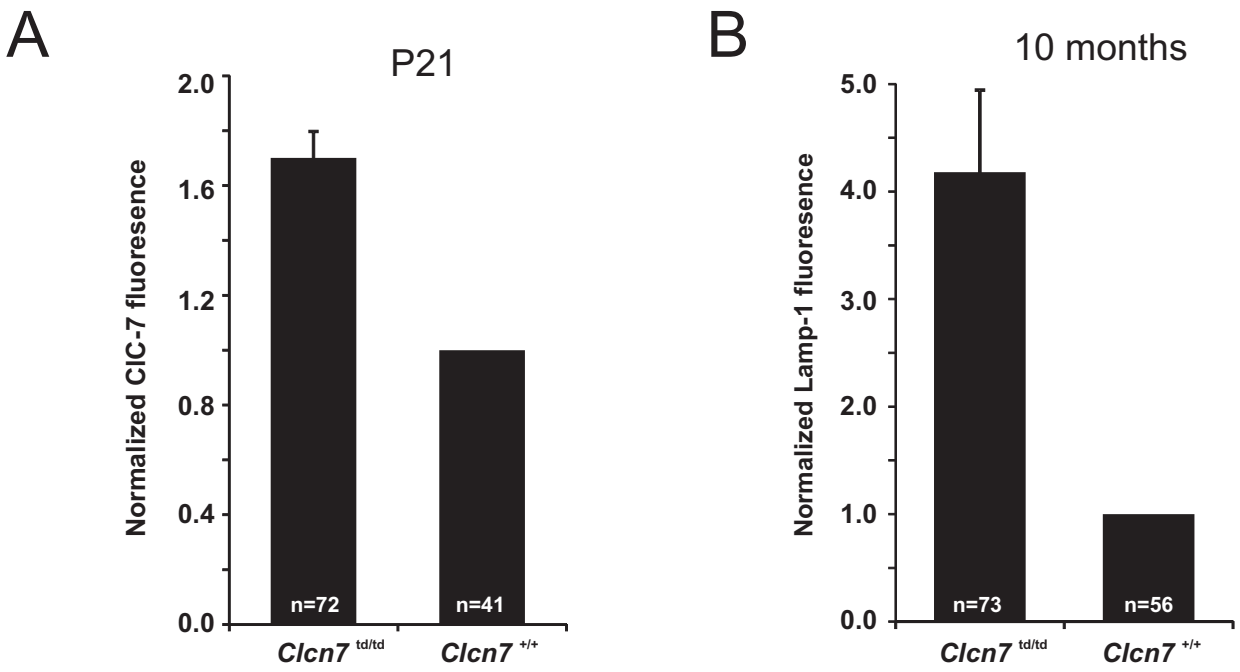

Figure E4. Quantification of abnormal lysosomal labelling. (**A**) About 70% increase of ClC-7 ^{td} fluorescence intensities in the somata of CA3 pyramidal neurons in *Clcn7* $^{td/td}$ mice compared to ClC-7 fluorescence intensities in *Clcn7* $^{+/+}$ mice at P21 (compare to main Figure 3A). Quantification was performed using ImageJ. A region of interest was placed around the cell bodies. Mean fluorescence intensities were determined and background subtracted. Quantifications were performed from 3 different animals per genotype including images shown in Figure 3. Normalization to images stained in parallel and acquired using identical settings. Total numbers of quantified cells are given. Error bars denote s.e.m. (**B**) Up to 4-fold increase of Lamp-1 fluorescence intensities in the somata of CA3 pyramidal neurons in *Clcn7* $^{td/td}$ mice at 10 months of age (compare to main Figure 3B). Autofluorescence of storage material which massively accumulates in lysosomal compartments in 10 months-old animals most likely contributes to the increased intensity. Quantification and normalization as in (A). Total numbers of quantified cells are given. Error bars denote s.e.m.

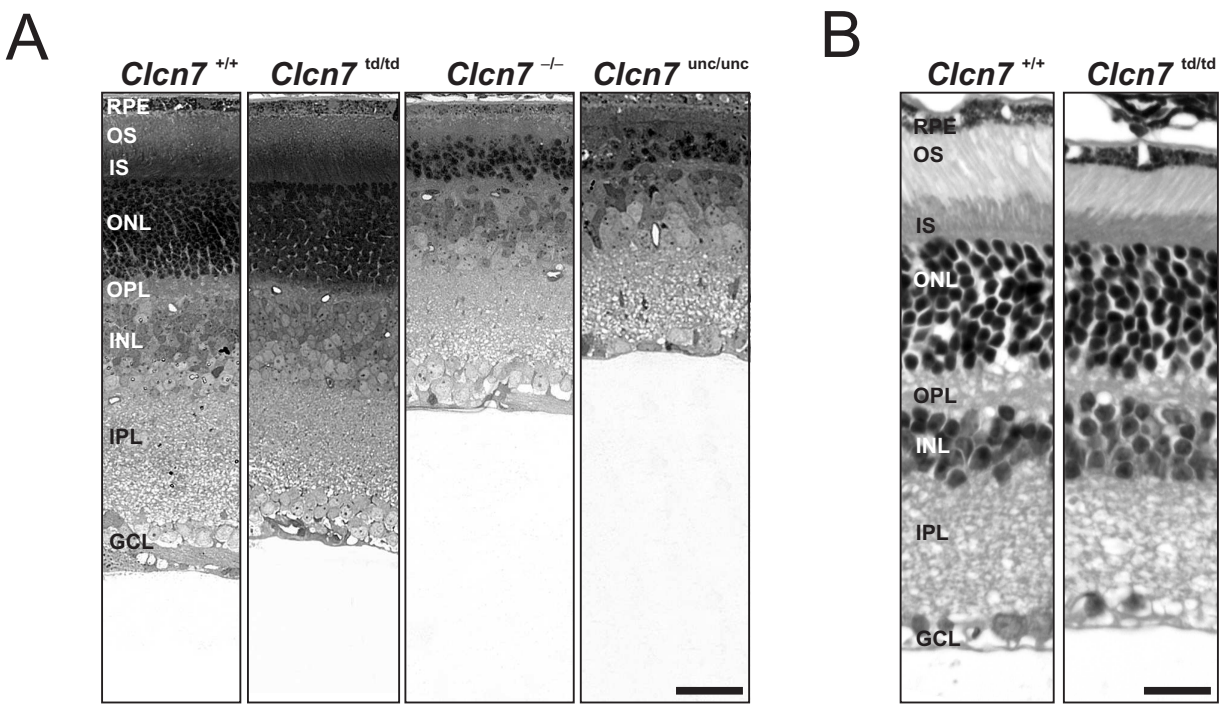

Figure E5. No retinal degeneration in *Clcn7*$^{td/td}$ mice. (**A**) Semi-thin sections of P28 retinae revealed degeneration of photoreceptor cells in the outer nuclear layer (ONL) and outer and inner segment (OS, IS, respectively) of *Clcn7*$^{unc/unc}$ and *Clcn7*$^{-/-}$, but not of *Clcn7*$^{td/td}$ mice (scale bar: 50 µm). (**B**) H&E staining on paraffin sections of the retina at 10 months of age. No obvious loss of photoreceptors in *Clcn7*$^{td/td}$ mice (n=2 animals each genotype). RPE, retinal pigment epithelium; OS, photoreceptor outer segments; IS, photoreceptor inner segments; ONL, outer nuclear layer; OPL, outer plexiform layer; INL, inner nuclear layer; IPL, inner plexiform layer; GCL, ganglion cell layer (scale bar: 100 µm).

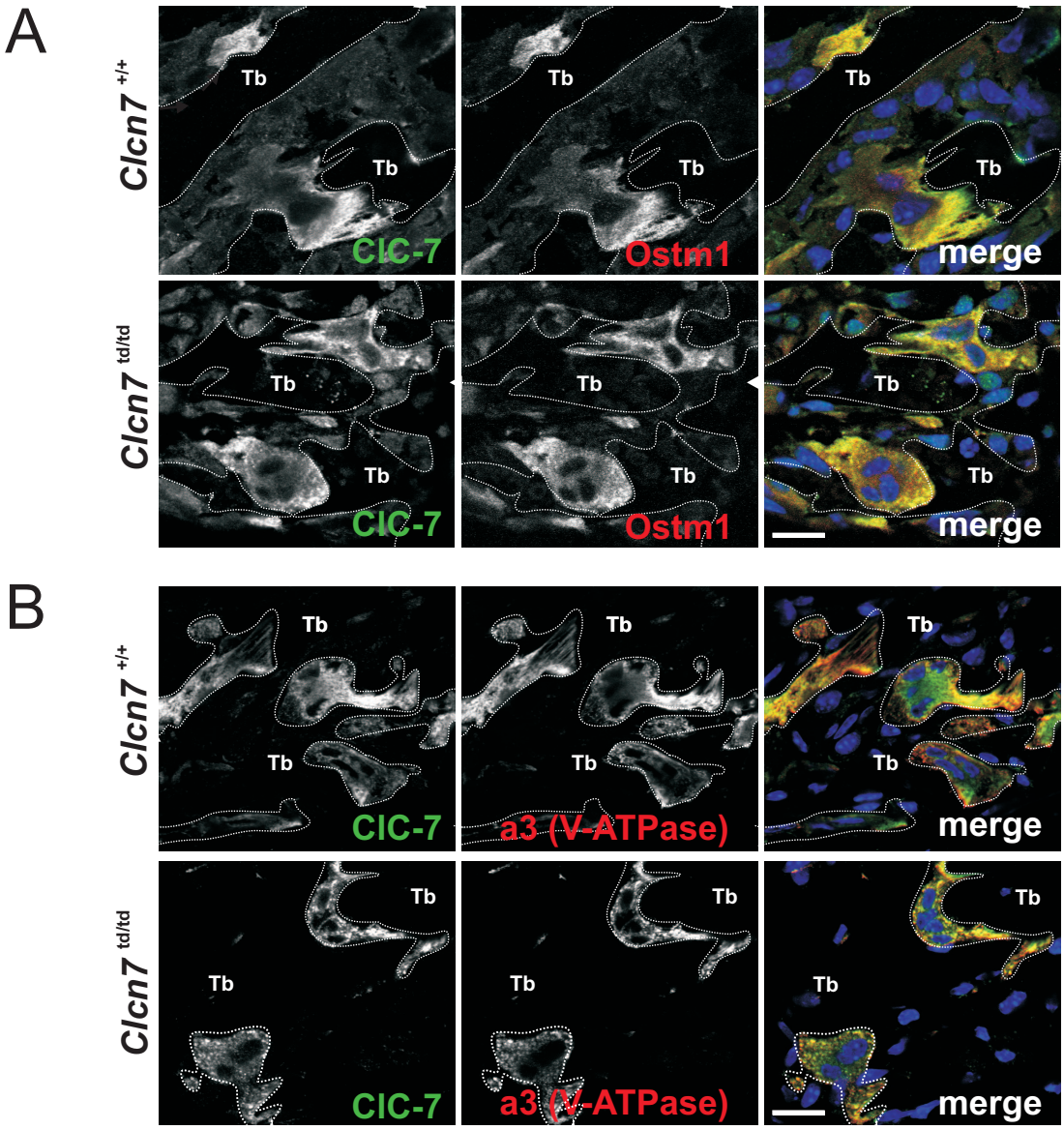

Figure E6. Localization of CIC-7^{td} and Ostm1 in *Clcn7*$^{td/td}$ tibia. (A) Immunostaining for ClC-7 (green) and Ostm1 (red) in bone. Both proteins showed dense overlapping staining in osteoclasts in areas that are partially opposed to trabecles (Tb) and represent ruffled borders (scale bar: 25 µm). (B) Co-localization of the a3 subunit of the V-ATPase (red) with WT ClC-7 and ClC-7td confirmed that both proteins were prominently found in the ruffled border and in intracellular compartments (dotted lines separate osteoclasts from bone tissue). DNA was stained with DAPI (scale bar: 25 µm).

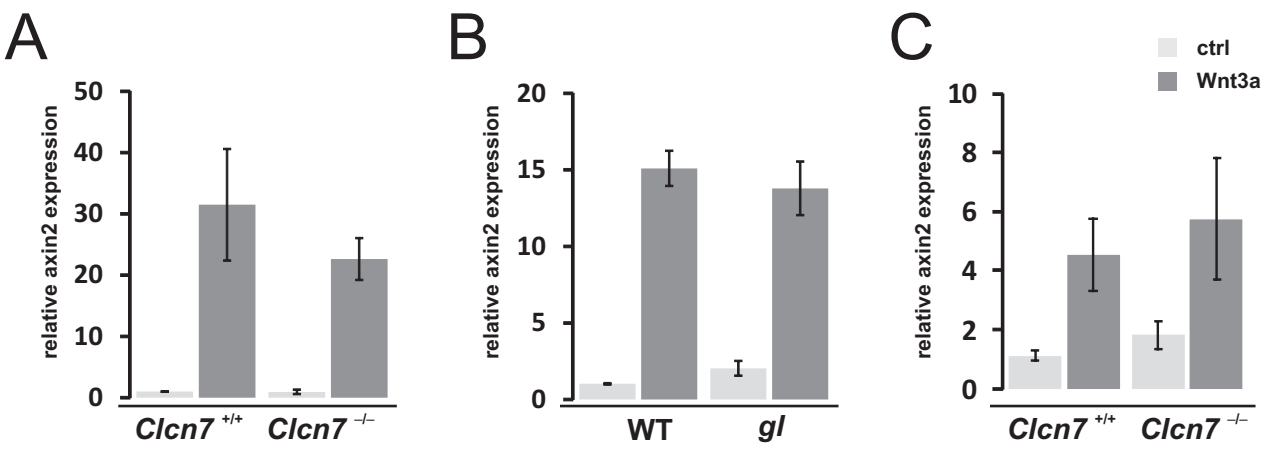

Figure E7. ClC-7/Ostm1-deficiency did not perturb Wnt signalling. WT and ClC-7-deficient (**A**) or gl (**B**) fibroblasts or WT and ClC-7-deficient melanocytes (**C**) were stimulated with rmWnt3a and expression levels of the Wnt target gene axin2 were determined by qRT-PCR. Experiments were performed with two (fibroblasts) and 6 (melanocytes) independent primary cell lines per genotype. Error bars denote s.e.m..

Expanded View

Mice

For the generation of *Clcn7*$^{td/td}$ mice 8 kb of mouse genomic sequence extending from exon 6 to 16 of *Clcn7* were amplified from R1 ES cells and cloned into pKO Scrambler plasmid 901 (Lexicon Genetics Incorporated) containing a dtA cassette (diphtheria toxin A cassette). A neomycin (neo) resistance cassette flanked by FRT sites was introduced between exon 7 and 8 to select for recombination in embryonic stem (ES) cells. Exon 11 was modified by insertion of the E312A mutation. The targeting construct was completely sequenced**.** Targeted R1 ES cells were screened by Southern blot analysis using *Bam*HI and an external 1.0-kb probe. Correctly targeted ES cells were injected into C57Bl/6 blastocysts. Chimeric animals were crossed with FLPe-recombinase-expressing 'deleter' mice and resulting heterozygous animals (*Clcn7*$^{+/td}$) were inbred to yield *Clcn7*$^{td/td}$. Exon 11 of the genomic *Clcn7*$^{td/td}$ gene was amplified with intronic primers and sequenced. Experiments were performed with mice in a mixed C57Bl/6-129/Svj genetic background, always using littermates as controls

Membrane preparation, tissue homogenates and immunoblot

For membrane preparation tissues were homogenized in PBS with protease inhibitors (Complete® protease inhibitor cocktail, Roche) and cleared two times by centrifugation at 1,000 x g for 10 min. Membranes were pelleted at 270,000 x g for 30 min and subsequently resuspended in PBS supplemented with protease inhibitors and 2% (w/v) SDS. For whole tissue homogenates organs were homogenized in PBS with 1% (v/v) NP-40 and protease inhibitors (Complete® protease inhibitor cocktail, Roche) and incubated for 30 min on ice. After centrifugation for 10 min at 20,800 x g the supernatant was used for SDS-PAGE. Equal amounts of protein were separated by SDS–PAGE and blotted onto nitrocellulose.

Histology and electron microscopy

Deeply anesthetized mice were perfused with 4% (w/v) PFA in PBS and isolated tissues were postfixed overnight at 4°C. Tibiae were decalcified for 4 days in 10% (w/v) EDTA in PBS and again postfixed. 3-µm paraffin sections of retina were used for H&E staining (old age), 8-µm paraffin sections of the brain were used for Nissl and periodic acid Schiff (PAS) staining and 8-µm cryosections for immunohistochemistry and lysosomal acid phosphatase assay. Lysosomal acid phosphatase activity *in situ* was determined using β-glycerophosphate as a substrate. Cryosections were incubated for 2 h at 37°C in 0.3% (w/v) sodium-β-glycerophosphate with 0.125% (w/v) lead nitrate in 50 mM acetate buffer pH 5.0. After washing, sections were stained with 0.1% (w/v) ammonium sulfide for 1 min. No staining was observed when substrate was omitted. For immunohistochemistry, sections were post fixed with 4% (w/v) PFA, permeabilized using 0.2% (v/v) Triton X-100 in PBS and blocked with 3% (w/v) BSA in PBS. Antibody incubation was in blocking buffer. For ClC-7, an antigen retrieval step (10 min in sodium citrate buffer, pH 6.0, at 95 °C) was included after fixation. For immunocytochemistry, fibroblasts were seeded onto glass coverslips, fixed for 12 min with 4% (w/v) PFA, treated with 30 mM glycine in PBS for 5 min, permeabilized with 0.1% (w/v) saponin and blocked with 3% (w/v) BSA in PBS. Confocal images were acquired with an LSM 510 (Zeiss) and ZEN software (Zeiss).

For electron microscopy, mice were perfused with 4% (w/v) PFA and 2.5% (v/v) glutaraldehyde in 0.1 M phosphate buffer (pH 7.4). Brains were cut in 150-µm sagittal sections with a vibratome. The eyes were opened at the crystalline lens and the vitreous humour removed. Tibiae were decalcified with 10% (w/v) EDTA in PBS for 3 to 4 days. Thin slices were prepared and postfixed in 2% (v/v) OsO_4, dehydrated and embedded in epon. Semi-thin sections (0.5 µm) were labelled with toluidine blue. Ultrathin sections (60 nm) were stained with uranyl acetate and lead citrate and examined with a Zeiss EM 902. Photographs were taken with a Megaview 3 Camera. Using the sealing zone as localization marker, the ruffled borders were graded *in situ* as absent, immature or mature with the experimenter blinded to the genotype.

Primary cell culture

Mouse adult fibroblasts from $Clcn7^{td/td}$, $Clcn7^{-/-}$ and WT mice were prepared by dissociation of tail biopsies with 0.2% (v/v) collagenase / 2U/ml dispase in PBS and cultured in DMEM containing 10% (v/v) fetal calf serum. Three independent cell lines from different animal were generated. For immunocytochemistry, fibroblasts were seeded onto glass coverslips and fixed. Melanocytes were isolated from dorsal skin of new-born pups by overnight dissociation of the epidermis in 0.25% Trypsin/EDTA solution (Life Technologies) at 4°C and cultured in melanocyte growth medium based on Ham's F12 (Life technologies) containing 20% (v/v) FBS, 1% (v/v) penicillin/streptomycin (both PAN-Biotech), 0.1 mM isobutylmethyl xanthine (Sigma-Aldrich), 10 µg/ml bovine pituitary extract (Life Technologies) and 48 nM 12-O-tetradecanoyl-phorbol-13-acetate (TPA, Sigma-Aldrich)

Determination of lysosomal pH

Lysosomal pH was measured by ratiometric fluorescence imaging of the pH sensor Oregon Green dextran 488 (Invitrogen) as described before . Primary cultures of fibroblasts were plated onto glass bottom life-cell dishes (MatTek) and loaded overnight with 0.5 mg/ml pH dye in growth medium. Cells were washed and Oregon Green dextran was chased into lysosomes for 2 h at 37°C in serum-supplemented growth medium. Ratiometric fluorescence images were acquired using an inverted microscope (Zeiss Axiovert 200 equipped with a 100x 1.30 NA oil immersion lens) connected to a Polychrom II monochromator (TILL photonics) at excitation wavelengths of 440 and 488 nm, respectively. The emitted light was filtered with a 535 ± 20-nm filter and captured with a Sensicam CCD camera (PCO). For each genotype, at least 3 different cells from 3 independent cell lines were measured in Ringer solution (in mM: 140 NaCl, 3 KCl, 2 K2HPO4, 1 CaCl2, 1 MgSO4, 5 HEPES, 10 glucose, pH 7.4). Image analysis was performed using a Fiji plug-in, in which regions of interest (ROI) were defined as areas above a defined fluorescence threshold in the acquired images at 488-nm excitation. The mean intensity ratio between 488- and 440-nm excitation was calculated for each ROI. At the end of each experiment, in situ pH calibration curves were obtained after treatment in isotonic K^+-based solutions (in mM: 5 NaCl, 115 KCl, 1.2 MgSO4, 10 glucose, 25 of either HEPES or MES, ranging in pH from 3.9 through 6.45) supplemented with 10 µM of both nigericin and monensin (both Sigma-Aldrich). Cells were equilibrated for at least 2 min for each pH value. The resulting fluorescence intensity ratio (488/440) as a function of pH was fit to a sigmoid and used to interpolate pH values from the experimental ratio data.

Determination of relative lysosomal chloride concentrations

Lysosomal chloride was measured by ratiometric fluorescence live cell imaging of MEQ/TMR-dextran (6-methoxy-N-ethylquinolinium iodide / tetramethylrhodamine-dextran) , that was targeted to lysosomes using a standard pulse-chase protocol. Primary cultures of fibroblasts were plated onto glass-bottom culture dishes (MatTek) and loaded for 1h with 20 mg/ml dye in growth medium. Cells were washed and MEQ/TMR-dextran chased into lysosomes for 2 h at 37°C in NaCl-reduced IMDM (Iscove's Modified Dulbecco's Medium; PAN-Biotech) with remaining [Cl^-] of 7 mM with NaCl substituted by Na-gluconate. Ratiometric fluorescence images at excitation wavelengths of 360 (MEQ) and 524 nm (TMR), respectively, were acquired using an inverted microscope (Zeiss Axiovert 200 equipped with a 100x 1.30 NA oil immersion lens) and an HC Tripleband Beamsplitter 403 497 574 (Semrock) connected to a Polychrom II monochromator (TILL Photonics) and a Lambda 10-2 emission filter wheel (Sutter Instruments). The emitted light was filtered with a 440 ± 20 nm (for MEQ) or 580 ± 20 nm filter (for TMR) and captured with a Sensicam CCD camera (PCO). For each genotype, 12 (+/+; td/td) or 7 (–/–) dishes with 10 different cells from 5 (+/+), 6 (td/td) or 2 (–/–) independent primary cell lines were measured in imaging buffer (in mM: Na-gluconate 135 mM Na-gluconate 5 KCl, 1 CaCl2, 1 MgCl2, 10 HEPES, 10 glucose, pH 7.4). Image analysis was performed with the Vision software package (TILL Photonics). For each cell, 10 lysosomes were chosen as regions of interest (ROI). The mean fluorescence intensity ratio between 360- and 524-nm excitation was calculated for each ROI after background subtraction.

Isolation of RNA and qRT-PCR

RNA was isolated from primary cells using the RNeasy mini kit (Qiagen) and transcribed to cDNA using SuperscriptII reverse transcriptase and random primers (Life technologies). qRT-PCR for axin2 was performed using RT² SYBR Green ROX qPCR Mastermix (Qiagen) with axin2-specific primers (forward: AGTCAGCAGAGGGACAGGAA; reverse CTTCGTACATGGGGAGCACT) in a StepOne Plus Cycler (Applied Biosystems). ß-Actin served as housekeeping gene (forward: tgtgatggtgggaatgggtcagaa; reverse: tgtggtgccagatcttctccatgt). The ΔΔCT method was used for analysis.

Supplementary Reference

Rodríguez CI, Buchholz F, Galloway J, Sequerra R, Kasper J, Ayala R, Stewart AF, Dymecki SM (2000) High-efficiency deleter mice show that FLPe is an alternative to Cre-loxP. *Nat Genet* **25:** 139-140